

Effect of bound-state dressing in laser-assisted radiative recombinationRobert A. Müller,^{1,2,*} Daniel Seipt,¹ Stephan Fritzsche,^{1,2} and Andrey Surzhykov¹¹*Helmholtz-Institute Jena, Fröbelstieg 3, 07743 Jena, Germany*²*Friedrich-Schiller-Universität Jena, Physikalisch-Astronomische Fakultät, Max-Wien-Platz 1, 07743 Jena, Germany*

(Received 17 June 2015; published 30 November 2015)

We present a theoretical study on the recombination of a free electron into the ground state of a hydrogenlike ion in the presence of an external laser field. Emphasis is placed on the effects caused by the laser dressing of the residual ionic bound state. To investigate how this dressing affects the total and angle-differential cross section of laser-assisted radiative recombination (LARR) we apply first-order perturbation theory and the separable Coulomb-Volkov continuum ansatz. Using this approach, detailed calculations are performed for low- Z hydrogenlike ions and laser intensities in the range from $I_L = 10^{12}$ to 10^{13} W/cm². It is seen that the total cross section as a function of the laser intensity is remarkably affected by the bound-state dressing. Moreover, the laser dressing becomes manifest as asymmetries in the angular distribution and the (energy) spectrum of the emitted recombination photons.

DOI: [10.1103/PhysRevA.92.053426](https://doi.org/10.1103/PhysRevA.92.053426)

PACS number(s): 34.50.Rk, 34.80.Lx, 32.80.Wr

I. INTRODUCTION

The recombination of a continuum electron into a bound state of an atom or ion accompanied by the emission of a photon is commonly called radiative recombination (RR). This fundamental process can be observed in many laboratory and astrophysical plasmas and in ion or electron storage rings [1–3]. The cross section of this process and the energy and angular distribution of the emitted recombination photons have been studied extensively over the past decades in both theory and experiment (see Refs. [3–5], and references therein). The characteristics of the emitted radiation may change remarkably after all if the electron and the nucleus are exposed to an external laser field. This additional field can accelerate or decelerate the electron before the recombination takes place and hence may broaden the spectrum and also modify the emission pattern of the recombination photons. It is of major importance to understand these effects since laser-assisted radiative recombination (LARR) is the third step in the process of high-harmonic generation [6,7]. Moreover, the external laser can cause a significant gain of the recombination yield, which may support the generation of neutral antimatter [8–10].

Laser-assisted radiative recombination was studied in a number of experiments (see, e.g., [11–15]). To understand the evidence found in these experiments a number of theoretical studies have been performed [6,7,16–18]. Up to now most of these studies had been carried out in the context of the strong-field approximation (SFA). In this theory, originally introduced by Keldysh [16], Faisal [17], and Reiss [18], the incident electron moves solely in the field of the external laser while the laser influence is neglected for the final bound electron. In recent decades several advancements of the SFA approach were proposed. In particular, an extension was developed to include the influence of the Coulomb field into the description of the incident electron [19]. More recently, first steps to include the laser influence on the residual bound state in the theory either perturbatively or by means of a Floquet expansion have been done [20–23]. Combining these advancements, Shchedrin and Volberg [24] performed a technical analysis of a theory where both the Coulomb

distortion of the continuum wave function and the perturbative dressing of the residual bound state were included. However, up to now no calculations of the differential LARR cross section have been presented respecting the influence of both potentials on both electron states. Moreover, the effect of bound-state dressing on two-color photoionization has been discussed [25], but it was not analyzed in the context of LARR. Therefore, in this paper we investigate in detail how the laser dressing of the bound state affects the photon emission in LARR. Our study is based on an S -matrix approach where we account for the influence of both fields (laser and Coulomb) in the representation of the initial and final electron states [21,24]. The incident electron is described by a separable Coulomb-Volkov wave function, the final one by a perturbative expansion of the laser-dressed bound state up to the first order. Using this approach, outlined in Sec. III, we present results for the angle-differential partial cross section in Sec. IV A and the total cross section in Sec. IV B. We find that the total cross section is typically enhanced due to the assisting laser field. Moreover, the bound-state dressing significantly affects the angular and the energy distribution of the recombination photons.

Atomic units are used throughout this paper ($e = m_e = \hbar = 1$), except when stated otherwise.

II. GEOMETRY OF LASER-ASSISTED RADIATIVE RECOMBINATION

Let us first discuss the geometry used for our description of LARR. Figure 1 displays an atom in its rest frame. The quantization axis (z axis) is chosen along the asymptotic momentum of the incident electron \mathbf{p} . The polarization vector $\boldsymbol{\epsilon}_L$ of the laser photon together with the electron momentum \mathbf{p} defines the xz plane. In this work we restrict ourselves to coplanar geometries in which the propagation direction \mathbf{k} of the recombination photon lies also in the xz plane. Therefore, we can characterize both the polarization of the laser photon $\boldsymbol{\epsilon}_L$ and the momentum \mathbf{k} of the recombination photon solely by their polar angles χ and θ_k with respect to the z axis.

III. THEORY

In this section we derive analytical expressions for the cross-section LARR. This cross section can be expressed

*Corresponding author: robert.alex.mueller@gmail.com

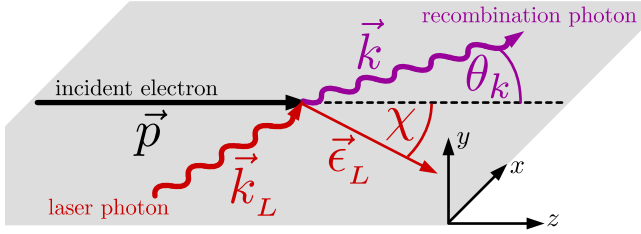


FIG. 1. (Color online) Geometry of laser-assisted radiative recombination. The z axis is given by the asymptotic momentum \mathbf{p} of the incoming electron. The xz plane is defined by \mathbf{p} and the laser polarization $\boldsymbol{\epsilon}_L$. The angle between these vectors is χ . The recombination photon is assumed to be emitted in the xz plane and therefore characterized by one angle θ_k .

in terms of the S -matrix element that is a measure for the probability that a continuum electron with momentum \mathbf{p} recombines into the bound state with quantum numbers (n, l, m) accompanied by the emission of a single recombination photon with frequency ω_k and polarization $\boldsymbol{\epsilon}_k^\lambda$:

$$S_{nlm} = -i \int_{-\infty}^{\infty} dt \langle \psi_{nlm}(\mathbf{r}, t) | e^{i(\omega_k t - \mathbf{k} \cdot \mathbf{r})} (\boldsymbol{\epsilon}_k^\lambda \cdot \nabla) | \psi_p(\mathbf{r}, t) \rangle. \quad (1)$$

Here λ is the helicity of the recombination photon and $\psi_p(\mathbf{r}, t)$ and $\psi_{nlm}(\mathbf{r}, t)$ are the initial continuum and final bound-state wave functions of the recombining electron. In the nonrelativistic regime these wave functions are taken as solutions of the time-dependent Schrödinger equation with the Hamiltonian

$$\hat{H}(t) = \frac{\hat{\mathbf{p}}^2}{2} - \frac{Z}{r} + \mathbf{A}_L(t) \cdot \hat{\mathbf{p}} + \frac{1}{2} \mathbf{A}_L(t)^2, \quad (2)$$

where $\hat{\mathbf{p}}$ is the electron momentum operator, Z the nuclear charge, and $\mathbf{A}_L(t)$ the vector potential of the external laser field with frequency ω_L and polarization $\boldsymbol{\epsilon}_L$. If the wavelength λ_L of this field is much larger than the size of the atom a_0 , the dipole approximation can be applied and the vector potential written as

$$\mathbf{A}_L(t) = \boldsymbol{\epsilon}_L A_L \cos(\omega_L t). \quad (3)$$

The corresponding electric field is then

$$\mathbf{E}_L(t) = \boldsymbol{\epsilon}_L E_L \sin(\omega_L t). \quad (4)$$

The laser intensity I_L in terms of the electric-field amplitude $E_L = \omega_L A_L$ is given by $I_L = c E_L^2 / 4\pi$.

A. Bound and continuum wave functions

In order to calculate the S matrix (1) of LARR we need to know the bound- and continuum-state wave functions $\psi_{nlm}(\mathbf{r}, t)$ and $\psi_p(\mathbf{r}, t)$. Since no analytical solutions are known for the Schrödinger equation with the Hamiltonian $\hat{H}(t)$ [Eq. (2)], we will show below how approximations can be derived for the initial continuum and final bound state of the electron.

1. Separable Coulomb-Volkov continuum states

In Eq. (1) $\psi_p(\mathbf{r}, t)$ describes the incident electron moving in the superposition of the atomic and the external laser potential.

A well-established approach to approximate such a wave function is to construct so-called separable Coulomb-Volkov continuum states [26]. We briefly recall here the derivation of this wave function that was originally introduced by Jain and Tzoar [26].

We assume that the electron motion in the continuum is mainly influenced by the external laser field. Therefore, the starting point for the construction of $\psi_p(\mathbf{r}, t)$ is the well-known Volkov wave function

$$\chi_p(\mathbf{r}, t) = e^{i\mathbf{p} \cdot \mathbf{r}} \exp \left[-i \left(E_i t + \frac{A_L}{\omega_L} \boldsymbol{\epsilon}_L \cdot \mathbf{p} \sin(\omega_L t) + \frac{A_L^2}{2} \int_{-\infty}^t \cos^2(\omega_L \tau) d\tau \right) \right], \quad (5)$$

which is the exact solution of the Schrödinger equation for an electron with kinetic energy E_i moving in a spatially homogeneous laser field switched on adiabatically at $t_0 \rightarrow -\infty$. To additionally account for the relatively weak influence of the Coulomb field we replace the plane term $\exp(i\mathbf{p} \cdot \mathbf{r})$ in Eq. (5) by the continuum wave function $\phi_p(\mathbf{r})$ of a hydrogenlike atom [27]

$$\begin{aligned} \psi_p(\mathbf{r}, t) &= \phi_p(\mathbf{r}) \exp \left[-i \left(E_i t + \frac{A_L}{\omega_L} \boldsymbol{\epsilon}_L \cdot \mathbf{p} \sin(\omega_L t) \right) \right] \\ &= (2\pi)^{-\frac{3}{2}} \exp \left[i \left(\mathbf{p} \cdot \mathbf{r} - E_i t - \frac{A_L}{\omega_L} \boldsymbol{\epsilon}_L \cdot \mathbf{p} \sin(\omega_L t) \right) \right] \\ &\quad \times \exp \left(\frac{\pi Z}{2p} \right) \Gamma(1 - iZ/p) \\ &\quad \times {}_1F_1[iZ/p, 1, i(pr - \mathbf{p} \cdot \mathbf{r})], \end{aligned} \quad (6)$$

but neglect all terms of the order $\sim A_L^2$ and higher. Here ${}_1F_1(a, b, z)$ and $\Gamma(z)$ are the confluent hypergeometric function and the Gamma function, respectively.

This approximation (6) is valid as long as the asymptotic electron momentum p is large compared to the momentum transferred to the electron by the laser field [26,28]. As can be seen from Eq. (2), this momentum transfer is quantified by the laser vector potential $\mathbf{A}_L(t)$. Therefore, the validity condition reads

$$\frac{A_L}{p} = \frac{A_L}{\sqrt{2E_i}} \ll 1. \quad (7)$$

For further discussion of the separable Coulomb-Volkov wave function and its validity we refer the reader to the literature (e.g., Refs. [26,28]).

2. Laser-dressed bound state

In the preceding section we derived the wave function $\psi_p(\mathbf{r}, t)$ for a continuum-state electron in a combined laser and Coulomb field. We obtained $\psi_p(\mathbf{r}, t)$ under the assumption that the atomic field is much weaker than the laser one. This is not the case if the electron is in a bound state. The intensity of the Coulomb field for the ground state of hydrogen is $I_C = (\alpha^2 e / a_0 m_e)^2 c^5 \epsilon_0 / 2 = 3.5 \times 10^{16} \text{ W/cm}^2$, which is much larger than any laser intensity discussed in this paper. To derive the bound-state wave function, therefore, we can treat the laser vector potential $\mathbf{A}_L(t)$ perturbatively. In first-order time-dependent perturbation theory $\psi_{nlm}(\mathbf{r}, t)$ can

be written as [29,30]

$$\begin{aligned} \psi_{nlm}(\mathbf{r}, t) = e^{-iE_n t} \left[\phi_{nlm}(\mathbf{r}) - \frac{A_L}{2} \sum_{n'l'm'} \left(\frac{e^{i\omega_L t}}{\omega_{n'n} + \omega_L} \right. \right. \\ \left. \left. + \frac{e^{-i\omega_L t}}{\omega_{n'n} - \omega_L} \right) \langle \phi_{n'l'm'} | \boldsymbol{\epsilon}_L \cdot \hat{\mathbf{p}} | \phi_{nlm} \rangle \phi_{n'l'm'}(\mathbf{r}) \right], \end{aligned} \quad (8)$$

where in the second term we restricted the summation to the bound-state solutions ϕ_{nlm} of the Schrödinger equation for hydrogenlike ions and $\omega_{n'n} = E_n - E_{n'}$ is the energy difference between the levels with principal quantum numbers n and n' . Additionally, we assume that the laser is not in resonance with any atomic transition.

Even though Eq. (8) holds for any bound state, we restrict ourselves to the $1s$ ground state, which is the dominant decay channel. Moreover if this capture into the K shell is assisted by an optical laser with frequency $\omega_L \ll 10.2 \text{ eV} \leq \omega_{n'1}$, the so-called soft-photon approximation is applicable [18,31] and we can neglect ω_L in the denominators in Eq. (8):

$$\begin{aligned} \psi_{1s}(\mathbf{r}, t) \equiv \psi_{100}(\mathbf{r}, t) = e^{-iE_1 t} \left(\phi_{100}(\mathbf{r}) - A_L \cos(\omega_L t) \right. \\ \left. \times \sum_{n'l'm'} \frac{1}{\omega_{n'1}} \langle \phi_{n'l'm'} | \boldsymbol{\epsilon}_L \cdot \hat{\mathbf{p}} | \phi_{100} \rangle \phi_{n'l'm'}(\mathbf{r}) \right). \end{aligned} \quad (9)$$

To further simplify this expression we apply the Heisenberg equation of motion for the unperturbed atomic Hamiltonian $\hat{H}_0 = \hat{\mathbf{p}}^2/2 - Z/r$ and rewrite the matrix element

$$\langle \phi_{n'l'm'} | \boldsymbol{\epsilon}_L \cdot \hat{\mathbf{p}} | \phi_{nlm} \rangle = i\omega_{n'n} \langle \phi_{n'l'm'} | \boldsymbol{\epsilon}_L \cdot \mathbf{r} | \phi_{nlm} \rangle \quad (10)$$

from velocity to length form. This allows us to perform the summation in Eq. (9) over the states $\phi_{n'l'm'}$ explicitly and to finally obtain

$$\psi_{1s}(\mathbf{r}, t) = e^{-iE_1 t} \phi_{100}(\mathbf{r}) [1 - iA_L \boldsymbol{\epsilon}_L \cdot \mathbf{r} \cos(\omega_L t)]. \quad (11)$$

The first term on the right-hand side of Eq. (11) is the unperturbed atomic wave function while the second term (dressing term) is the perturbative correction due to the external laser. This correction is proportional to $A_L r$ and hence the approximation is valid as long as $A_L r \ll 1$. In our calculations for hydrogen we consider a characteristic length $r = a_0 = 1 \text{ a.u.}$

B. Evaluation of the S -matrix element

With the wave functions describing the electron before [Eq. (6)] and after [Eq. (11)] the capture in hand, we can calculate the S matrix of LARR. By inserting these wave functions into Eq. (1) we obtain for the recombination into the ground state

$$\begin{aligned} S_{1s} &= -i \int_{-\infty}^{\infty} dt \langle \psi_{1s}(\mathbf{r}, t) | e^{i\omega_k t} (\boldsymbol{\epsilon}_k^\lambda \cdot \nabla) | \psi_p(\mathbf{r}, t) \rangle \\ &= -i \int_{-\infty}^{\infty} dt \int_{\mathbb{R}^3} d^3\mathbf{r} e^{i(E_1 - E_i + \omega_k)t} [e^{i\kappa \sin(\omega_L t)} \\ &\quad + iA_L \boldsymbol{\epsilon}_L \cdot \mathbf{r} \cos(\omega_L t) e^{i\kappa \sin(\omega_L t)}] \phi_{100}^*(\mathbf{r}) (\boldsymbol{\epsilon}_k^\lambda \cdot \nabla) \phi_p(\mathbf{r}), \end{aligned} \quad (12)$$

where we defined $\kappa = A_L \boldsymbol{\epsilon}_L \cdot \mathbf{p} / \omega_L$. Moreover, we applied the dipole approximation for the interaction of the emitted recombination photon and the electron. In this approximation $\mathbf{k} \cdot \mathbf{r} \ll 1$, which is well justified for all cases discussed in this paper.

The time integration in the second line of Eq. (12) can be performed analytically if we make use of the Jacobi-Anger expansion and its first derivative with respect to t :

$$e^{i\kappa \sin(\omega_L t)} = \sum_{N=-\infty}^{\infty} J_N(\kappa) e^{iN\omega_L t}, \quad (13a)$$

$$\cos(\omega_L t) e^{i\kappa \sin(\omega_L t)} = \frac{1}{\kappa} \sum_{N=-\infty}^{\infty} N J_N(\kappa) e^{iN\omega_L t}, \quad (13b)$$

where $J_N(\kappa)$ is the Bessel function of the first kind. The time-integrated S matrix for the recombination into the ground state then can be written as

$$\begin{aligned} S_{1s} &= -2\pi i \sum_{N=-\infty}^{\infty} \delta(E_1 - E_i + \omega_k - N\omega_L) \\ &\quad \times M^{(N)}(A_L, \boldsymbol{\epsilon}_L, \mathbf{p}, Z), \end{aligned} \quad (14)$$

where the δ function provides for energy conservation and E_1 is the binding energy of the ground state of the hydrogenlike ion. In this notation the photon number N can be interpreted as the number of laser photons that are absorbed ($N > 0$) or emitted ($N < 0$) by the electron. Therefore, the S matrix (14) is an infinite sum of partial matrix elements $M^{(N)}(A_L, \boldsymbol{\epsilon}_L, \mathbf{p}, Z)$, each corresponding to a particular number N of exchanged laser photons. These partial matrix elements can be written

$$M^{(N)}(A_L, \boldsymbol{\epsilon}_L, \mathbf{p}, Z) = J_N(\kappa) \left(M_{RR}(\mathbf{p}, Z) + \frac{N\omega_L}{\boldsymbol{\epsilon}_L \cdot \mathbf{p}} M_{dr}(\mathbf{p}, Z) \right) \quad (15)$$

as the sum of two constituent matrix elements $M_{RR}(\mathbf{p}, Z)$ and $M_{dr}(\mathbf{p}, Z)$,

$$\begin{aligned} M_{RR}(\mathbf{p}, Z) &= B \boldsymbol{\epsilon}_k^\lambda \cdot \mathbf{e}_p \frac{p - iZ}{(p^2 + Z^2)^2} \left(i \frac{Z}{p} - 1 \right) \frac{iZ/p}{i \frac{Z}{p} + 1}, \quad (16a) \\ M_{dr}(\mathbf{p}, Z) &= B \left(1 - i \frac{Z}{p} \right) \frac{(Z - ip)^{-2iZ/p}}{(p^2 + Z^2)^{2-iZ/p}} \\ &\quad \times \left(\boldsymbol{\epsilon}_L \cdot \boldsymbol{\epsilon}_k^\lambda - 2(\boldsymbol{\epsilon}_L \cdot \mathbf{e}_p)(\boldsymbol{\epsilon}_k^\lambda \cdot \mathbf{e}_p) \frac{2p^2 - ipZ}{Z^2 + p^2} \right), \end{aligned} \quad (16b)$$

where $B = 2\pi i \sqrt{2Z^5} \exp(\pi Z/2p) \Gamma(1 - iZ/p)$ and $\mathbf{e}_p = \mathbf{p}/p$ is the unit vector that points the initial asymptotic electron momentum. The derivation of these constituent matrix elements is shown in Appendix A.

Equation (16a) represents the standard matrix element of laser-free radiative recombination, where $A_L = 0$. In this case $\kappa = 0$ and we get $S_{1s} = -2\pi i \delta(E_1 - E_i + \omega_k) M_{RR}(\mathbf{p}, Z)$. The constituent matrix element $M_{dr}(\mathbf{p}, Z)$ has its origin in the laser-dressing contribution to the bound-state wave function (11). By setting $M_{dr}(\mathbf{p}, Z) = 0$, therefore, we can

readily investigate results for bound states uninfluenced by the laser field. This splitting of the partial matrix element $M^{(N)}$ into two parts is consistent with the findings of Shchedrin and Volberg [24].

C. Differential and total LARR cross section

Up to now we discussed expressions (15) and (16) for the partial matrix element $M^{(N)}$ of laser-assisted radiative recombination into the ground state of a hydrogenlike system. We can use these expressions to calculate the total and angle-differential LARR cross sections. For example, the angle-differential partial cross section for the recombination of an electron accompanied by an emission or absorption of N laser photons is given by

$$\frac{d\sigma_{1s}^{(N)}}{d\Omega_k} = \frac{4\pi^2}{c^3 p} \omega_k(N) \sum_{\lambda} |M^{(N)}|^2. \quad (17)$$

Here c is the speed of light in vacuum and Ω_k the solid angle into which the recombination photon is emitted. Moreover, we assume that the polarization of the recombination photon remains unobserved and hence sum over the helicity λ .

The frequency ω_k of the recombination photon in Eq. (17) is given by the conservation law

$$\omega_k(N) = E_i - E_1 + N\omega_L. \quad (18)$$

Since ω_k is always positive, the photon number has to yield the inequality $N \leq N_{\min} = (E_i - E_1)/\omega_L$.

From Eq. (17) we can obtain the total cross section by integrating over the solid angle Ω_k and summing over the photon number N from $\lceil N_{\min} \rceil$ to infinity:

$$\sigma_{1s} = \frac{4\pi^2}{c^3 p} \sum_{N=N_{\min}}^{\infty} \sum_{\lambda} \int d\Omega_k \omega_k(N) |M^{(N)}|^2. \quad (19)$$

This cross section characterizes the probability to produce a hydrogen ion by LARR. However, the sum in Eq. (19) is infinite and not all terms contribute equally to the total cross section. If we perform a stationary-phase analysis of Eq. (12) (following Refs. [32,33]) we find that the partial matrix element $M^{(N)}$ is nearly zero if $|N|$ exceeds the cutoff photon number

$$N_{\text{cut}} = A_L p / \omega_L. \quad (20)$$

Accordingly, if $N_{\text{cut}} < |N_{\min}|$ we can take $N_{\min} \rightarrow -\infty$ without changing the result significantly.

IV. RESULTS AND DISCUSSION

A. Differential partial cross section

In the past LARR has been discussed mainly within the SFA [19,34]. The laser influence on the bound state is neglected in this approximation. Anyhow, we expect from previous attempts [24] that the emission pattern and energy distribution of the recombination photons is affected by the bound-state dressing. Therefore, we use our theory to investigate these effects and perform calculations for the angle-differential partial cross section.

In Fig. 2 we show the differential partial cross section of laser-assisted recombination into the $1s$ state of hydrogen. The

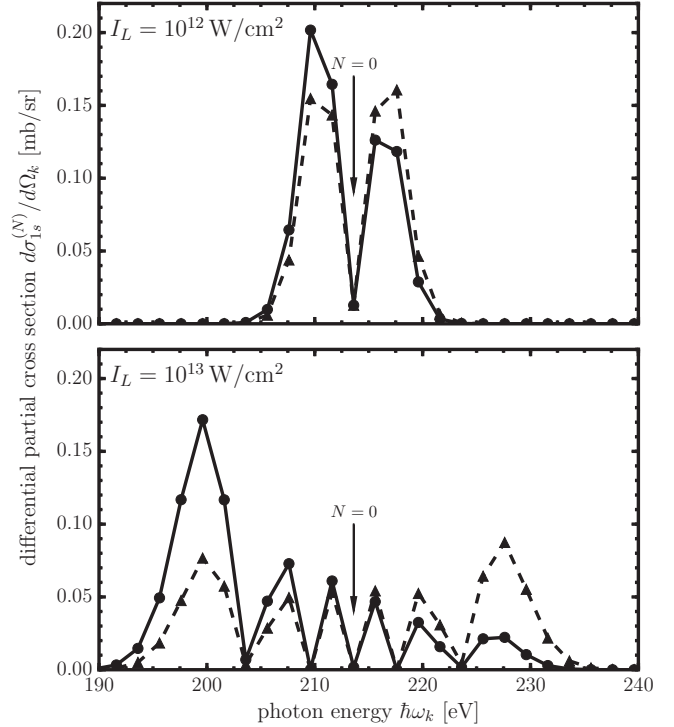


FIG. 2. Angle-differential partial cross section (17) for the laser-assisted recombination of an $E_i = 200$ -eV electron and a hydrogen nucleus ($Z = 1$) as a function of the recombination photon energy $\omega_k(N)$. The calculations have been performed for a photon emission angle $\theta_k = 175^\circ$ and a laser polarization angle $\chi = 135^\circ$. The laser parameters are $\hbar\omega_L = 2$ eV and $I_L = 10^{12}$ W/cm 2 (top) and $I_L = 10^{13}$ W/cm 2 (bottom). The dashed lines and triangles refer to the results where the dressing of the target bound states is neglected. The spectrum is discrete and the lines are only shown to guide the eye.

calculations have been carried out for a fixed photon emission angle $\theta_k = 175^\circ$ and an external laser ($\hbar\omega_L = 2$ eV) with two different laser intensities $I_L = 10^{12}$ W/cm 2 (top panel) and $I_L = 10^{13}$ W/cm 2 (bottom panel). Results are shown with (circles) and without (triangles) incorporation of the laser dressing of the bound state. Of course, the LARR cross section is only defined at the discrete energies $\omega_k(N)$ shown in Eq. (18) and the solid and dashed lines are only shown to guide the eye.

It can be seen in Fig. 2 that the spectrum is not just a single line, as it would be for the laser-free radiative recombination, but a distribution of photon energies. The width of this distribution increases from about 18 eV for $I_L = 10^{12}$ W/cm 2 to 46 eV for $I_L = 10^{13}$ W/cm 2 . This intensity-dependent broadening of the spectrum can be understood from the scaling of cutoff photon number N_{cut} that becomes larger as the intensity increases [cf. Eq. (20)].

As can be seen from Fig. 2, the dressed and undressed results behave quite differently as a function of $\omega_k(N)$. The results obtained without bound-state dressing are almost symmetric around the field-free photon energy where $N = 0$. A slight increase of $d\sigma_{1s}^{(N)}/d\Omega_k$ towards higher photon energies is caused by the prefactor $\omega_k(N)$ in Eq. (17) that scales linearly but weakly with N . If, in contrast, the bound-state dressing is included in the computations, the photon distribution becomes

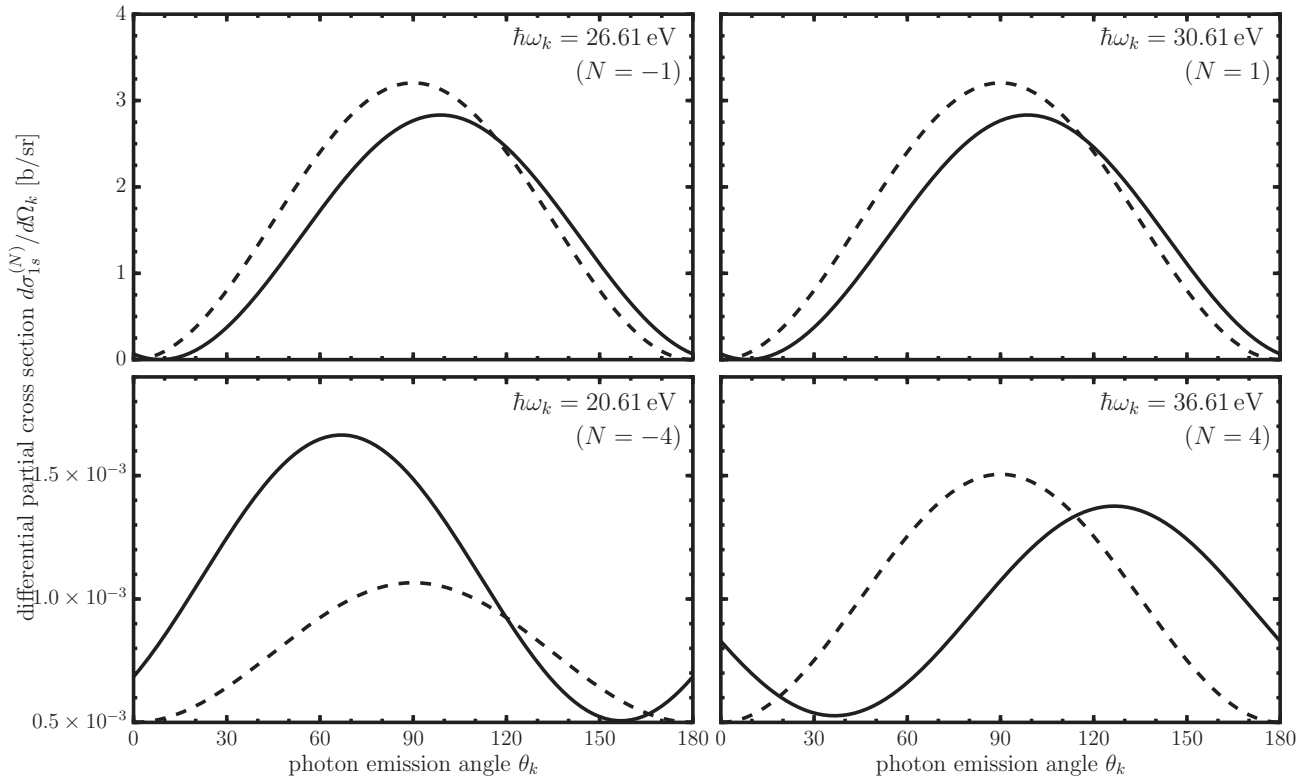


FIG. 3. Angle-differential partial cross section for the laser-assisted recombination of an $E_i = 15$ -eV electron into the ground state of hydrogen ($Z = 1$) as a function of the photon emission angle θ_k . The assisting laser has an intensity of $I_L = 10^{13}$ W/cm² and the frequency $\hbar\omega_L = 2$ eV. Its polarization angle is $\chi = 65^\circ$. Results are shown for four different recombination photon energies: In the top row $\hbar\omega_k(N = -1) = 26.61$ eV (left) and $\hbar\omega_k(N = 1) = 30.61$ eV (right) while in the bottom row $\hbar\omega_k(N = -4) = 20.61$ eV (left) and $\hbar\omega_k(N = 4) = 36.61$ eV (right). In all panels we show results obtained including (solid lines) and omitting (dashed lines) the bound-state dressing in comparison.

strongly asymmetric. This can be explained by the fact that the contribution of $M_{dr}(\mathbf{p}, Z)$ increases with N , as can be seen from Eq. (15). For higher intensities, sidebands with larger photon numbers are visible and therefore the asymmetries become more pronounced.

Figure 2 displays the spectral distribution (17) of the recombination photons for a fixed photon emission angle θ_k . In order to investigate the θ_k dependence of $d\sigma_{1s}^{(N)}/d\Omega_k$ we present in Fig. 3 the angular distribution of the recombination photons emitted during the recombination of 15-eV electrons into the $1s$ state of hydrogen. The calculations were performed for a laser with intensity $I_L = 10^{13}$ W/cm², frequency $\hbar\omega_L = 2$ eV, and different energies of the recombination photons: $\hbar\omega_k(N = -1) = 26.61$ eV (top left panel), $\hbar\omega_k(N = 1) = 30.61$ eV (top right panel), $\hbar\omega_k(N = -4) = 20.61$ eV (bottom left panel), and $\hbar\omega_k(N = 4) = 36.61$ eV (bottom right panel). Again we compare results obtained including (solid lines) and neglecting (dashed lines) the bound-state dressing. As can be seen from Fig. 3, the emission pattern of the recombination photons is symmetric around 90° if the bound-state wave function is assumed to be uninfluenced by the laser. This behavior is easily understood by setting $M_{dr}(\mathbf{p}, Z) = 0$ in Eq. (15). The LARR cross section (17) can be written then as $d\sigma_{1s}^{(N)} \sim \sum_\lambda |\epsilon_k^\lambda \mathbf{e}_p|^2 = 1 - |\mathbf{e}_p \mathbf{e}_k|^2 = \sin^2 \theta_k$ (see Ref. [27]). This angular distribution is independent of the photon number N and therefore the same for all recombination

photon energies (cf. Fig. 3). However, a different angular behavior occurs if the bound-state dressing is taken into account. The constituent matrix element $M_{dr}(\mathbf{p}, Z)$ contains additional angular-dependent terms that lead to an asymmetric shift of the angular distribution. This shift becomes larger for higher photon numbers N that enter Eq. (15) as a prefactor of $M_{dr}(\mathbf{p}, Z)$. However, as can be seen from Fig. 2 and Eq. (20), large- N contributions become visible only if I_L or E_i is sufficiently high.

B. Total cross section of LARR

In the previous section we showed that the differential partial cross section (17) of LARR may be influenced remarkably by the laser dressing of the residual bound atomic state. This effect becomes more pronounced for higher photon numbers N . As we have shown in Sec. III C, however, only the channels with $|N| \leq N_{\text{cut}}$ contribute to the cross section. Since N_{cut} depends on the energy of the incident electron E_i and the laser intensity I_L , we expect that also the total cross section as a function of E_i and I_L is influenced by the bound-state dressing. In order to study this we display in Fig. 4 the total cross section (19) of LARR as a function of the incident electron energy for three different nuclear charges Z . For our calculations we set the laser intensity $I_L = 10^{13}$ W/cm² and the frequency $\hbar\omega_L = 2$ eV. Again we compare results

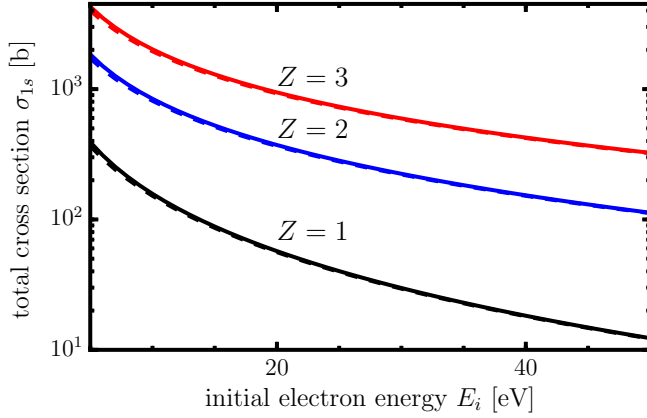


FIG. 4. (Color online) Total cross section of laser-assisted radiative recombination into the ground state of a hydrogenlike ion as a function of the initial electron energy E_i for three different nuclear charges ($Z = 1$, black line; $Z = 2$, blue line; and $Z = 3$, red line). The calculations have been performed for a laser with the intensity $I_L = 10^{13} \text{ W cm}^{-2}$, laser photon energy $\hbar\omega = 2 \text{ eV}$ and a polarization angle $\chi = 90^\circ$. We show results calculated with laser-dressed bound-state wave functions (solid lines) and results where the bound-state dressing is neglected (dashed lines).

obtained with the laser dressing being neglected (dashed lines) and taken into account (solid lines). From this comparison we see that in the latter case the LARR cross section is enhanced. This difference between the two cases (with and without bound-state dressing) vanishes for increasing kinetic energies of the incident electron. For example, for $Z = 1$ in the low-energy regime at $E_i = 5 \text{ eV}$, σ_{1s} is increased by a factor of 1.07. For $E_i = 30 \text{ eV}$ this factor is only 1.01.

Up to now we have discussed the total LARR cross section σ_{1s} as a function of the initial electron energy E_i for different nuclear charges Z and $I_L = 10^{13} \text{ W/cm}^2$. Beyond that we expect that σ_{1s} can also depend on the laser intensity. Figure 5 shows the total LARR cross section (19) as a function of the laser intensity I_L , again for three different nuclear charges Z . Moreover, we present our results for two sets of initial electron energies $E_i = 5 \text{ eV} \times Z^2$ and $E_i = 10 \text{ eV} \times Z^2$. We apply this scaling of E_i to better illustrate how the dressing effects depend on Z . Because the laser-free cross section is defined solely by the Sommerfeld parameter $\nu = \sqrt{Z^2/2E_i}$, the Z dependence of the total cross section at a fixed E_i/Z^2 comes from the bound-state dressing only. Similarly to before, we see in Fig. 5 that the effect of bound-state dressing decreases with increasing energy E_i . Moreover, the effect of bound-state dressing is decreased for higher nuclear charges Z . This is due to the stronger binding of the electrons in the ground state of the hydrogenlike ion.

It can be seen in Fig. 5 that the bound-state dressing causes a qualitative different behavior of the total LARR cross sections. The results obtained without bound-state dressing are independent of the laser intensity while the full calculations increase linearly with I_L . To explain this behavior we insert the partial matrix element (15) into Eq. (19) and perform the summation over N . Since for the discussed scenario $N_{\text{cut}} < |N_{\text{min}}|$ is satisfied, the sum can be extended to negative

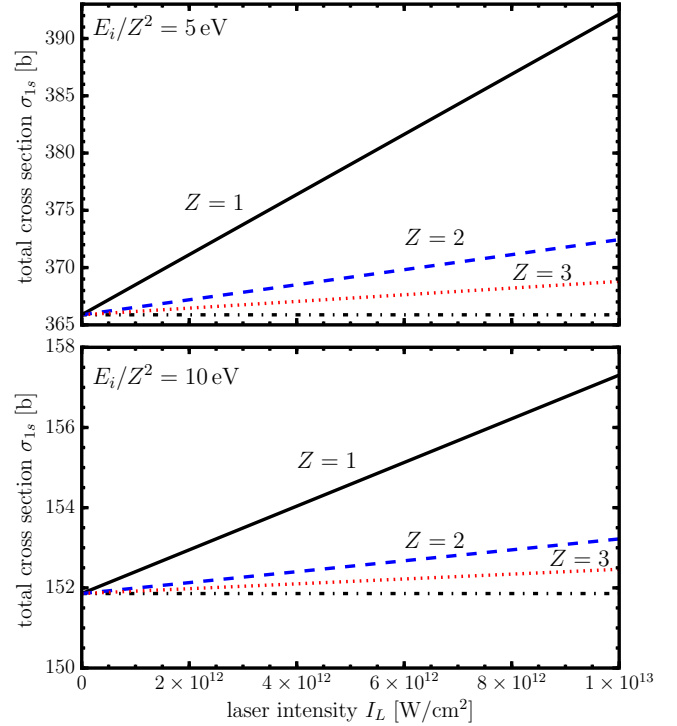


FIG. 5. (Color online) Total cross section for laser-assisted radiative recombination into the ground state of a hydrogenlike ion as a function of the laser intensity I_L for $\omega_L = 2 \text{ eV}$ and three different nuclear charges ($Z = 1$, black solid line; $Z = 2$, blue dashed line; and $Z = 3$, red dotted line). The initial electron energy is normalized with respect to the nuclear charge such that $E_i/Z^2 = 5 \text{ eV}$ (top) and $E_i/Z^2 = 10 \text{ eV}$ (bottom). The polarization angle is $\chi = 90^\circ$. For comparison the laser-free case and the result obtained with undressed bound-state wave functions are shown (black dot-dashed lines in the top and bottom, respectively).

infinity. This enables us to use

$$\sum_{N=-\infty}^{\infty} J_N^2(\kappa) = 1, \quad (21a)$$

$$\sum_{N=-\infty}^{\infty} N^2 J_N^2(\kappa) = \frac{\kappa^2}{2}, \quad (21b)$$

$$\sum_{N=-\infty}^{\infty} N^{2j+1} J_N^2(\kappa) = 0 \quad \text{for } j \in \mathbb{N}_0 \quad (21c)$$

and to obtain the total cross section in the form

$$\begin{aligned} \sigma_{1s} = & \frac{4\pi^2}{c^3 p} \sum_{\lambda} \int d\Omega_k \left[(E_i - E_1) |M_{RR}|^2 \right. \\ & \left. + \frac{E_L^2}{2\omega_L^2} [(E_i - E_1) |M_{dr}|^2 + (\boldsymbol{\epsilon}_L \cdot \mathbf{p}) \text{Re}(M_{RR}^* M_{dr})] \right]. \end{aligned} \quad (22)$$

From this expression we see that the total cross section scales quadratically with the laser electric-field amplitude E_L and therefore linearly with the laser intensity I_L . If in contrast the bound-state dressing is neglected ($M_{dr} = 0$), the total cross

section σ_{1s} does not depend on I_L . Moreover, in this case Eq. (22) reduces to the standard laser-free RR cross section. This implies that, within the present model, the assisting laser affects the total cross section solely via the bound-state dressing.

V. SUMMARY

In this paper we presented a theoretical study of the recombination of a free electron into the ground state of a hydrogenlike ion in the field of an external laser. We put special emphasis on the effects that arise from the laser dressing of the bound ionic state. In order to investigate how this dressing affects the total and angle-differential LARR cross sections we applied the S -matrix theory and the dipole approximation for the coupling of the electron to electromagnetic fields. Within this theory the incident electron in the combined field of the laser and the nucleus is described by a separable Coulomb-Volkov wave function. To account for the influence of the laser field on the final bound state we used time-dependent perturbation theory up to the first order.

Based on the developed approach, we performed calculations for the differential partial cross section $d\sigma_{1s}^{(N)}/d\Omega_k$ as a function of the emission angle θ_k and the energy $\omega_k(N)$ of the recombination photon. We found that $d\sigma_{1s}^{(N)}/d\Omega_k$ is symmetric around $\theta_k = 90^\circ$ if the bound-state dressing is neglected while the full calculations show an asymmetric shift of the angular distribution. Comparing the energy distribution of the emitted recombination photons obtained either with or without bound-state dressing, we see remarkable differences, especially for higher photon numbers N .

Moreover, results have been obtained for the total cross section as a function of the incident electron energy E_i and the laser intensity I_L . We found that, within the validity of our theory, the total cross section of LARR may be enhanced if the bound-state dressing is taken into account. It was shown analytically that this enhancement is linear in I_L . However, if the bound-state dressing is neglected, the total LARR cross section is constant with respect to I_L and coincides with the total cross section of laser-free radiative recombination.

Laser-assisted atomic processes have gained increasing interest in recent years, especially those using intense laser fields. While it has been common to neglect dressing effects on bound atomic states, this study stresses their importance for higher intensities.

ACKNOWLEDGMENT

R.A.M. acknowledges support of the Studienstiftung des Deutschen Volkes.

APPENDIX: DERIVATION OF THE CONSTITUENT MATRIX ELEMENTS

To derive closed expressions for the constituent matrix elements we insert the wave functions $\psi_p(\mathbf{r}, t)$ (6) and $\psi_{1s}(\mathbf{r}, t)$ (11) into the general equation for the S matrix (12). After time integration we find

$$M_{RR}(\mathbf{p}, Z) = \int_{\mathbb{R}^3} d^3\mathbf{r} \phi_{100}(\mathbf{r})(\boldsymbol{\epsilon}_k \cdot \nabla)\psi_p(\mathbf{r}), \quad (\text{A1a})$$

$$M_{dr}(\mathbf{p}, Z) = \int_{\mathbb{R}^3} d^3\mathbf{r} \boldsymbol{\epsilon}_L \cdot \mathbf{r} \phi_{100}(\mathbf{r})(\boldsymbol{\epsilon}_k \cdot \nabla)\psi_p(\mathbf{r}). \quad (\text{A1b})$$

To perform the spatial integration analytically we multiply the integrands by $1 = e^{i\mathbf{k}\cdot\mathbf{r}}|_{\mathbf{k}=0}$ and obtain

$$M_{RR}(\mathbf{p}, Z) = 2^6 \pi^3 B(\boldsymbol{\epsilon}_k \cdot \nabla_k) \mathcal{I}(Z, \mathbf{p}, \mathbf{k})|_{\mathbf{k}=0}, \quad (\text{A2a})$$

$$M_{dr}(\mathbf{p}, Z) = -i 2^6 \pi^3 B(\boldsymbol{\epsilon}_L \cdot \nabla_k)(\boldsymbol{\epsilon}_k \cdot \nabla_k) \mathcal{I}(Z, \mathbf{p}, \mathbf{k})|_{\mathbf{k}=0}, \quad (\text{A2b})$$

where B has been introduced in Eq. (16) and ∇_k is the gradient with respect to the components of \mathbf{k} . The remaining integral over the spatial coordinates is now reduced to a standard atomic integral $\mathcal{I}(Z, \mathbf{p}, \mathbf{k})$ that can be found, e.g., in Ref. [27], yielding

$$\begin{aligned} \mathcal{I}(Z, \mathbf{p}, \mathbf{k}) &= \int_{\mathbb{R}^3} \frac{d^3\mathbf{r}}{r} e^{i(\mathbf{p}-\mathbf{k})\cdot\mathbf{r}-Zr} {}_1F_1(iZ/p, 1, i(\mathbf{p}-\mathbf{k})\cdot\mathbf{r}) \\ &= 4\pi \frac{[k^2 + (Z - ip)^2]^{-iZ/p}}{[(\mathbf{p}-\mathbf{k})^2 + Z^2]^{1-iZ/p}}. \end{aligned} \quad (\text{A3})$$

Using this relation and performing the \mathbf{k} derivatives in (A2), we obtain the results shown in Eq. (16):

$$M_{RR}(\mathbf{p}, Z) = B \boldsymbol{\epsilon}_k^\lambda \cdot \mathbf{e}_p \frac{p - iZ}{(p^2 + Z^2)^2} \left(\frac{i\frac{Z}{p} - 1}{i\frac{Z}{p} + 1} \right)^{iZ/p}, \quad (\text{A4a})$$

$$\begin{aligned} M_{dr}(\mathbf{p}, Z) &= B \left(1 - i\frac{Z}{p} \right) \frac{(Z - ip)^{-2iZ/p}}{(p^2 + Z^2)^{2-iZ/p}} \\ &\quad \times \left(\boldsymbol{\epsilon}_L \cdot \boldsymbol{\epsilon}_k^\lambda - 2(\boldsymbol{\epsilon}_L \cdot \mathbf{e}_p)(\boldsymbol{\epsilon}_k^\lambda \cdot \mathbf{e}_p) \frac{2p^2 - ipZ}{Z^2 + p^2} \right). \end{aligned} \quad (\text{A4b})$$

- [1] H. Yamaguchi, M. Ozawa, K. Koyama, K. Masai, J. S. Hiraga, M. Ozaki, and D. Yonetoku, *Astrophys. J. Lett.* **705**, L6 (2009).
 [2] R. Schuch, T. Quinteros, M. Pajek, Y. Haruyama, H. Danared, G. Hui, G. Andler, D. Schneider, and J. Starker, *Nucl. Instrum. Methods Phys. Res. Sect. B* **79**, 59 (1993).

- [3] Y. Hahn, *Rep. Prog. Phys.* **60**, 691 (1997).
 [4] A. Surzhykov, S. Fritzsche, and T. Stöhlker, *J. Phys. B* **35**, 3713 (2002).
 [5] S. Fritzsche, A. Surzhykov, and T. Stöhlker, *Phys. Rev. A* **72**, 012704 (2005).

- [6] P. B. Corkum, *Phys. Rev. Lett.* **71**, 1994 (1993).
- [7] M. Lewenstein, Ph. Balcou, M. Yu. Ivanov, A. L'Huillier, and P. B. Corkum, *Phys. Rev. A* **49**, 2117 (1994).
- [8] M. L. Rogelstad, F. B. Yousif, T. J. Morgan, and J. B. A. Mitchell, *J. Phys. B* **30**, 3913 (1997).
- [9] C. Wesdorp, F. Robicheaux, and L. D. Noordam, *Phys. Rev. Lett.* **84**, 3799 (2000).
- [10] E. S. Shuman, R. R. Jones, and T. F. Gallagher, *Phys. Rev. Lett.* **101**, 263001 (2008).
- [11] U. Schramm, J. Berger, M. Grieser, D. Habs, E. Jaeschke, G. Kilgus, D. Schwalm, A. Wolf, R. Neumann, and R. Schuch, *Phys. Rev. Lett.* **67**, 22 (1991).
- [12] A. Scrinzi, N. Elander, and A. Wolf, *Z. Phys. D* **34**, 185 (1995).
- [13] U. Schramm, T. Schüssler, D. Habs, D. Schwalm, and A. Wolf, *Hyperfine Interact.* **99**, 309 (1996).
- [14] T. Mohamed, G. Andler, M. Fogle, E. Justiniano, S. Madzunkov, and R. Schuch, *Phys. Rev. A* **83**, 032702 (2011).
- [15] M. Möller, Y. Cheng, S. D. Khan, B. Zhao, K. Zhao, M. Chini, G. G. Paulus, and Z. Chang, *Phys. Rev. A* **86**, 011401(R) (2012).
- [16] L. V. Keldysh, *Zh. Eksp. Teor. Fiz.* **47**, 1945 (1965) [*Sov. Phys. JETP* **20**, 1307 (1965)].
- [17] F. H. M. Faisal, *J. Phys. B* **6**, L89 (1973).
- [18] H. Reiss, *Phys. Rev. A* **22**, 1786 (1980).
- [19] A. Jaroń, J. Z. Kamiński, and F. Ehlötzky, *Phys. Rev. A* **61**, 023404 (2000).
- [20] S. Bivona, G. Bonanno, R. Burlon, and C. Leone, *Phys. Rev. A* **76**, 031402(R) (2007).
- [21] S.-M. Li and U. D. Jentschura, *J. Phys. B* **42**, 185401 (2009).
- [22] A. N. Zheltukhin, N. L. Manakov, A. V. Flegel, and M. V. Frolov, *JETP Lett.* **94**, 599 (2011).
- [23] A. N. Zheltukhin, A. V. Flegel, M. V. Frolov, N. L. Manakov, and A. F. Starace, *J. Phys. B* **45**, 081001 (2012).
- [24] G. Shchedrin and A. Volberg, *J. Phys. A* **44**, 245301 (2011).
- [25] A. Cionga, V. Florescu, A. Maquet, and R. Taïeb, *Phys. Rev. A* **47**, 1830 (1993).
- [26] M. Jain and N. Tzoar, *Phys. Rev. A* **18**, 538 (1978).
- [27] L. D. Landau and E. M. Lifshitz, *Quantum Mechanics: Non-Relativistic Theory* (Butterworth-Heinemann, Oxford, 1991).
- [28] P. Cavaliere, G. Ferrante, and C. Leone, *J. Phys. B* **13**, 4495 (1980).
- [29] C. J. Joachain, N. J. Kylstra, and R. M. Potvliege, *Atoms in Intense Laser Fields* (Cambridge University Press, Cambridge, 2011).
- [30] F. W. Byron, Jr., P. Francken, and C. J. Joachain, *J. Phys. B* **20**, 5487 (1987).
- [31] P. Francken and C. J. Joachain, *Phys. Rev. A* **35**, 1590 (1987).
- [32] D. Seipt and B. Kämpfer, *Phys. Rev. A* **89**, 023433 (2014).
- [33] M. Y. Kuchiev and V. N. Ostrovsky, *Phys. Rev. A* **61**, 033414 (2000).
- [34] W. Becker, S. Long, and J. K. McIver, *Phys. Rev. A* **50**, 1540 (1994).